Universal lower bounds on energy and momentum diffusion in liquids

K. Trachenko ⬤,[1] M. Baggioli,[2] K. Behnia,[3] and V. V. Brazhkin[4]

[1]*School of Physics and Astronomy, Queen Mary University of London, Mile End Road, London E1 4NS, United Kingdom*
[2]*Instituto de Fisica Teorica UAM/CSIC, c/ Nicolas Cabrera 13-15, Cantoblanco, 28049 Madrid, Spain*
[3]*Laboratoire de Physique et Etude des Matériaux (CNRS–Sorbonne Université–ESPCI), PSL Research University, 75005 Paris, France*
[4]*Institute for High Pressure Physics, RAS, 108840 Troitsk, Moscow, Russia*

Thermal energy can be conducted by different mechanisms including by single particles or collective excitations. Thermal conductivity is system-specific and shows a richness of behaviors currently explored in different systems, including insulators, strange metals, and cuprate superconductors. Here, we show that despite the seeming complexity of thermal transport, the thermal diffusivity α of liquids and supercritical fluids has a lower bound that is fixed by fundamental physical constants for each system as $\alpha_m = \frac{1}{4\pi} \frac{\hbar}{\sqrt{m_e m}}$, where m_e and m are electron and molecule masses. The newly introduced elementary thermal diffusivity has an absolute lower bound dependent on $\hbar$ and the proton-to-electron mass ratio only. We back up this result by a wide range of experimental data. We also show that theoretical minima of α coincide with the fundamental lower limit of kinematic viscosity ν_m. Consistent with experiments, this points to a universal lower bound for two distinct properties—energy and momentum diffusion—and a surprising correlation between the two transport mechanisms at their minima. We observe that α_m gives the minimum on the phase diagram except in the vicinity of the critical point, whereas ν_m gives the minimum on the entire phase diagram.

I. INTRODUCTION

Thermal energy can propagate by radiation, convection, and conduction. The latter phenomenon refers to the travel of heat in matter in the absence of particle flow. Thermal energy can be carried by phonons and electronic quasiparticles in solids and liquids or molecular collisions in gases [1,2]. Although the two mechanisms of heat transfer by collective excitations or particles are conceptually simple, they can interestingly interact with other processes and give rise to a rich variety of behaviors. This is currently explored in a variety of materials, including insulators, strange metals, and cuprate superconductors, where new mechanisms are invoked to explain the experimental data (see, e.g., Refs. [3–6]). More recently, bounds on thermal conductivity and other properties were discussed, with the view that identifying and understanding these bounds is important for fundamental physics, predictions for theory and experiment, as well as searching and rationalizing universal behavior [3–13]. These bounds are based on uncertainty relations and limits due to quantum physics.

Thermal conductivity is defined by the static Fourier equation, $J_Q = \kappa \frac{\partial T}{\partial x}$, where J_Q is the heat current density and $\frac{\partial T}{\partial x}$ is the temperature gradient in the x direction. This equation is the thermal counterpart of the Ohm equation and defines κ as a linear response to a static temperature gradient. Thermal diffusivity is described by the heat equation [14,15]

$$\frac{\partial T}{\partial t} = \alpha \frac{\partial^2 T}{\partial x^2}, \qquad (1)$$

where $\alpha = \frac{\kappa}{\rho c_p}$ is thermal diffusivity, ρ is density, and c_p is heat capacity per mass unit. α plays the role of the diffusion constant quantifying the propagation of thermal energy.

The transport coefficients κ and α vary in a wide range, and they depend strongly on the system, temperature, and pressure. Here, we consider α in liquid and supercritical states of matter, and we show that despite these variations, α at its *minimum*, α_m, universally attains a value

$$\alpha_m = \frac{1}{4\pi} \frac{\hbar}{\sqrt{m_e m}}, \qquad (2)$$

where m_e and m are electron and molecule masses, and we back up this result by experimental data.

We subsequently introduce the elementary thermal diffusivity $\iota = \alpha_m m$, similarly to the elementary viscosity [16], with the universal minimum set by fundamental constants as

$$\iota_m = \frac{\hbar}{4\pi} \left(\frac{m_p}{m_e} \right)^{\frac{1}{2}}, \qquad (3)$$

where m_p is the proton mass.

We finally show that the theoretical minima of thermal diffusivity coincide with the minima of a physically distinct quantity, the kinematic viscosity ν_m discussed recently [16], and that the experimental ratio ν_m/α_m is close to 1 and is in the range 0.4–1.7. Fundamentally, this closeness can be explained by observing that both α and ν at their minima are governed by the "ultraviolet" (UV) properties such as Bohr radius and Debye frequency. This suggests a wider universality of properties at their fundamental limit. We finally observe that (i) ν_m gives the minimum on the entire phase diagram of matter, and (ii) α_m gives the minimum on the phase diagram except in the vicinity of the critical point.

It is notable that the universal results (2) and (3) fixing the minimum for each system apply to the liquid state. Indeed, liquid properties are considered to be system-specific because interactions are strong and depend on the system. This circumstance is viewed to disallow a possibility of calculating liquid properties in general form [17]. A fundamental problem of liquid description is related to the absence of a small parameter [18]: interactions and atomic displacements in liquids are both large, and this combination precludes using theories developed for gases and solids. For example, the theoretical calculation and understanding of liquid energy and heat capacity has remained a long-standing problem in research and teaching [19], and it started to lift only recently when a new understanding of collective excitations in liquids came in [18]. For these reasons, there is no tractable microscopic theory of thermal conductivity in liquids [20]. In view of these problems, the existence of universal bound for α_m (2) and ι_m (3) in liquids is notable, as is the closeness of the lower bounds of α_m and ν_m despite the fundamental physical distinction between energy and momentum diffusion and very different ways of measuring α and ν.

II. RESULTS AND DISCUSSION

A. Derivation of the thermal diffusivity minimum

In this section, we derive the thermal diffusivity at its minimum. We start our discussion with the thermal diffusivity due to ionic motion, and we will comment on the electron conductivity later. We will see that Eqs. (2) and (3) emerge from connecting thermal diffusivity at the minimum to quantum-mechanical properties of condensed matter phases including the Bohr radius and Rydberg energy.

It is useful first to show the experimental data showing the minima. We have collected available experimental data [21] of κ in several noble (Ar, Ne, He, and Kr), molecular (N$_2$, H$_2$, O$_2$, CO$_2$, CH$_4$ C$_2$H$_6$, and CO), and network fluids (H$_2$O). Our selection includes industrially important supercritical fluids such as CO$_2$ and H$_2$O [22]. We have calculated $\alpha = \frac{\kappa}{\rho c_p}$ using the experimental values of c_p and ρ at respective temperatures, and we show both κ and α in Fig. 1. For some fluids, we show the data at two different pressures. The low pressure was chosen to be far above the critical pressure so that the data are not affected by near-critical anomalies. The highest pressure was chosen to (a) make the pressure range considered as wide as possible, and (b) be low enough in order to see the minima in the temperature range available experimentally. We observe that κ and α universally have minima. We also observe that κ can have weak maxima at low temperature related to the competition between the increase of heat capacity due to phonon excitations in the quantum regime and the decrease of the phonon mean free path l as in solids. In H$_2$O, the broad maximum is related to water-specific anomalies including broad structural transformation between differently coordinated states.

We now move to the reason why κ and α have minima in liquids as a function of temperature. In solids, the thermal conductivity κ can be written as $\kappa = cvl$, where c is the specific heat per volume unit [1], v is the speed of sound, l is the phonon mean free path, and we dropped the numerical
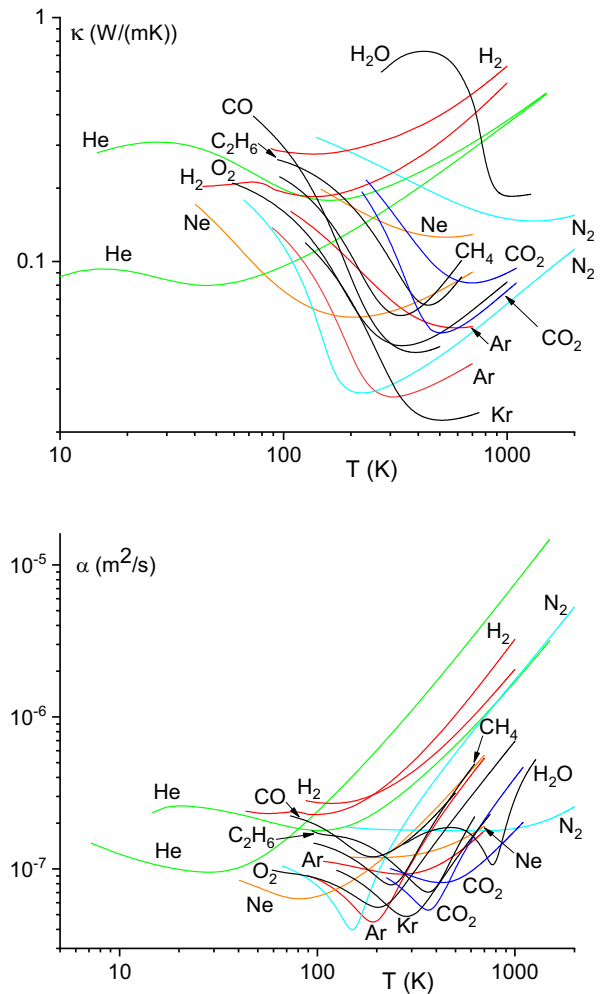

FIG. 1. Experimental thermal conductivity κ (top) and thermal diffusivity α (bottom) of noble, molecular, and network liquids [21] showing minima. κ and α for Kr, O$_2$, H$_2$O, CH$_4$, C$_2$H$_6$, and CO are shown for pressure $P = 30$, 30, 70, 20, 20, and 20 MPa, respectively. κ and α for Ar, Ne, He, N$_2$, H$_2$, and CO$_2$ are shown at two pressures each: 20 and 100 MPa for Ar, 50 and 300 MPa for Ne, 20 and 100 MPa for He, 10 MPa and 500 MPa for N$_2$, 50 MPa and 100 MPa for H$_2$, and 30 and 90 MPa for CO$_2$. The minimum at higher pressure is above the minimum at lower pressure for each fluid.

factor on the order of unity. Then, the diffusion constant is given by

$$\alpha = vl. \tag{4}$$

In gases, α can be written in the same way as (4), but—and this reflects the difference between heat transfer in solids and gases—v in (4) corresponds to the average velocity of gas molecules and l to the molecule free path [2].

The minimum of α is due to the crossover between the liquidlike and gaslike regimes of particles dynamics, which we qualify below. Molecular motion in low-temperature liquids combines solidlike oscillations around quasiequilibrium positions and diffusive jumps to new positions, enabling liquid flow. These jumps are due to temperature-induced molecular jumps over an energy barrier set by the interaction with

other molecules, resulting in the exponential temperature dependence of viscosity. The jumps are characterized by the liquid relaxation time, τ, i.e., the average time between the molecular jumps [23]. The collective excitations in liquids (we refer to these as phonons or phononlike modes in a wider sense [18]) consist of one longitudinal mode and two transverse modes propagating above the threshold value in k-space [18,24]. The temperature increase has two effects on α in Eq. (4). First, the phonon mean free path l decreases. Second, the speed of sound decreases as it does in solids. However, the decrease of v and l cannot continue indefinitely due to the UV cutoff in condensed matter phases: l is limited by the interatomic separation a at the Mott-Ioffe-Regel (MIR) limit, and τ is limited by the elementary vibration period, commonly approximated by the Debye vibration period τ_D.

An important effect related to reaching the UV cutoff is that a further temperature increase results in the qualitative change of particle dynamics [18,25,26]. On further temperature increase, the oscillatory component of molecular motion is lost, and molecules start moving in a purely diffusive manner. At high temperature and/or low density, molecules gain enough energy to move a distance l_p without collisions with velocity v_t, where l_p is the particle mean free path and v_t is the thermal velocity. l_p and v_t both increase with temperature. Therefore, α in Eq. (4) has a minimum. The same argument leading to a minimum applies to $\kappa = c\rho\alpha$. In the liquidlike regime, ρ and c are monotonically decreasing functions of temperature [18], hence the minima of α and κ can take place at different temperature.

If the temperature is increased at pressure below the critical point, the system crosses the boiling line and undergoes a liquid-gas transition. As a result, α and κ undergo a sharp change at the phase transition, rather than showing a smooth minimum as in Fig. 1. To avoid the effects related to the phase transition, we need to consider the supercritical state. Here, the Frenkel line [18,25,26] formalizes the qualitative change of molecular dynamics from combined oscillatory and diffusive to purely diffusive. The Frenkel line touches the boiling line slightly below the critical point and extends to arbitrarily high temperature and pressure on the phase diagram. At sufficiently high pressure and temperature, it runs nearly parallel to the boiling line in the logarithmic (pressure, temperature) coordinates [25]. The location of minima of different properties such as viscosity or thermal conductivity may depend on the path taken on the phase diagram. As a result, the minima may deviate from the Frenkel line depending on the path [18].

Before evaluating α_m, we first see how well we can estimate κ at the minimum, κ_m, using our approach. When l becomes comparable to a at the minimum, the velocity v can be evaluated as $v = \frac{a}{\tau_D}$ because the time for a molecule to move a distance a in this regime is given by the characteristic timescale set by τ_D. Recalling that c featuring in $\kappa = cvl$ is the temperature derivative of energy density [1], $c = \frac{c_v}{a^3}$, where c_v is the heat capacity per atom at constant volume (the derivative is taken at constant volume) and a^{-3} is the concentration. At the minimum, c_v is close to $2k_B$, reflecting the disappearance of two transverse modes at the dynamical crossover [18,24]. Setting $l = a$, $v = \frac{a}{\tau_D} = \frac{1}{2\pi}\omega_D a$, where ω_D

is Debye frequency, gives

$$\kappa_m = \frac{1}{\pi}\frac{k_B\,\omega_D}{a}. \tag{5}$$

Taking the typical values of $a = 3$–6 Å and $\frac{\omega_D}{2\pi}$ on the order of 1 THz, we find κ_m in the range 0.05–0.09 $\frac{W}{mK}$, providing an order of magnitude estimation of κ_m consistent with the experimental minima in Fig. 1(a). This sets the stage for our later calculation of thermal diffusivity at its minimum using fundamental physical constants.

We note that the minimum of κ in Fig. 1(a) is lower than thermal conductivity in low-κ solids such as SnSe ($\kappa = 0.23 \frac{W}{mK}$), where it is considered as "ultralow" [27].

We also observe that high pressure reduces a and increases ω_D. Equation (5) predicts that κ_m increases with pressure as a result, in agreement with the experimental behavior in Fig. 1. We note that (4) applies in the regime where l is larger than a, and in this sense our evaluation of the conductivity minimum is an order-of-magnitude estimation, as are our other results below. In this regard, we note that theoretical models can only describe a dilute gas limit where perturbation theory applies [2], but not in the regime where l is comparable to a and where the energy of intermolecular interaction is comparable to the kinetic energy. In view of theoretical issues, we consider our evaluation useful. In addition to being informative, an order-of-magnitude evaluation is perhaps unavoidable if a complicated property such as thermal conductivity is to be expressed in terms of fundamental constants only.

We are now ready to evaluate α at its minimum, α_m. As discussed above, l at the minimum is $l \approx a$. The speed of sound v in the Debye model is $v = \frac{a}{\tau_D}$ (at the crossover where τ becomes comparable to the time it takes the molecule to move a distance a and where $\tau \approx \tau_D$ as discussed above, v becomes approximately equal to thermal velocity). Using $l = a$ and $v = \frac{a}{\tau_D} = \frac{1}{2\pi}a\omega_D$ in (4) gives

$$\alpha_m = \frac{1}{2\pi}\omega_D a^2. \tag{6}$$

The energy diffusion constant α_m in (6) can now be related to fundamental physical constants by recalling that the properties defining the UV cutoff in condensed matter can be expressed in terms of fundamental constants [16]. For the benefit of the reader and later discussion, we reproduce the brief derivation below. Two relevant quantities are Bohr radius, a_B, setting the characteristic scale of interparticle separation on the order of angstrom,

$$a_B = \frac{4\pi\epsilon_0\hbar^2}{m_e e^2}, \tag{7}$$

and the Rydberg energy, $E_R = \frac{e^2}{8\pi\epsilon_0 a_B}$ [1], setting the characteristic scale for the cohesive energy in condensed matter phases on the order of several eV:

$$E_R = \frac{m_e e^4}{32\pi^2\epsilon_0^2\hbar^2}, \tag{8}$$

where e and m_e are electron charge and mass.

The characteristic phonon energy $\hbar\omega_D$ is related to the cohesive energy E, $\frac{\hbar\omega_D}{E}$, as

$$\frac{\hbar\omega_D}{E} = \left(\frac{m_e}{m}\right)^{\frac{1}{2}}, \qquad (9)$$

which, up to a factor close to 1, follows from approximating $\hbar\omega_D$ as $\hbar(\frac{E}{ma^2})^{\frac{1}{2}}$, taking the ratio $\frac{\hbar\omega_D}{E}$, and using $a = a_B$ from (7) and $E = E_R$ from (8).

Combining (6) and (9) gives

$$\alpha_m = \frac{1}{2\pi}\frac{Ea^2}{\hbar}\left(\frac{m_e}{m}\right)^{\frac{1}{2}}. \qquad (10)$$

The parameters a and E in (10) are set by their characteristic scales a_B and E_R as discussed earlier. Using $a = a_B$ from (7) and $E = E_R$ from (8) in (10) gives a remarkably simple equation for α_m as in Eq. (2), which we reproduce below for convenience:

$$\alpha_m = \frac{1}{4\pi}\frac{\hbar}{\sqrt{m_e m}}. \qquad (11)$$

Equation (11) is the main result of this paper. The same result for α_m in (11) can be obtained without explicitly using a_B and E_R in (10). The cohesive energy, or the characteristic energy of electromagnetic interaction, is

$$E = \frac{\hbar^2}{2m_e a^2}. \qquad (12)$$

Using (12) in (10) gives (11).

We now analyze (11) and its implications. α_m contains $\hbar$ and electron and molecule masses only. m characterizes the molecules involved in heat transfer. m_e characterizes electrons setting the intermolecular interactions. The quantum origin of α_m, signified by $\hbar$ in (11), is due to the quantum nature of interparticle interactions.

The mass m in (11) is $m = Am_p$, where A is the atomic weight and m_p is the proton mass. The inverse square root dependence $\alpha_m \propto \frac{1}{\sqrt{A}}$ interestingly implies that for different liquids α_m varies by a factor of about 10 only. Setting $m = m_p$ ($A = 1$) for H in (11) [similarly to (7) and (8) derived for the H atom] gives the fundamental thermal diffusivity in terms of $\hbar$, m_e, and m_p as

$$\alpha_m = \frac{1}{4\pi}\frac{\hbar}{\sqrt{m_e m_p}} \approx 10^{-7}\,\frac{\mathrm{m}^2}{\mathrm{s}}. \qquad (13)$$

For the lightest element, H, Eq. (13) gives the maximal value of α_m. It is interesting to ask what quantity has an absolute minimum. If we define the "elementary conductivity" ι ("iota") equivalent to the elementary viscosity [16] as $\iota = \alpha_m m$, Eq. (11), we obtain $\iota = \frac{\hbar}{4\pi}(\frac{m}{m_e})^{\frac{1}{2}}$. ι has the absolute minimum, ι_m, for H, where m is the proton mass m_p:

$$\iota_m = \frac{\hbar}{4\pi}\left(\frac{m_p}{m_e}\right)^{\frac{1}{2}} \qquad (14)$$

and is on the order of $\hbar$.

Equation (14) interestingly involves the proton-to-electron mass ratio, one of few dimensionless combinations of fundamental constants of importance in a variety of areas [28]. Together with the fine-structure constant, this ratio has a

TABLE I. Theoretical (th) and experimental (exp) values for the thermal diffusivity α_m and the kinematic viscosity ν_m at the minima. All the quantities are displayed in units of $\times 10^8$ m^2/s except for the last ratio, which is dimensionless.

	$\alpha_m^{\mathrm{th}} = \nu_m^{\mathrm{th}}$	α_m^{exp}	ν_m^{exp}	ν_m/α_m
Ar (20 MPa)	3.4	4.5	5.9	1.3
Ar (100 MPa)	3.4	9.3	7.7	0.8
Ne (50 MPa)	4.8	6.4	4.6	0.7
Ne (300 MPa)	4.8	11.9	6.5	0.6
He (20 MPa)	10.7	9.5	5.2	0.6
He (100 MPa)	10.7	17.9	7.5	0.4
Kr (30 MPa)	2.3	4.9	5.2	1.1
N$_2$ (10 MPa)	4.1	4.0	6.5	1.6
N$_2$ (500 MPa)	4.1	17.8	12.7	0.7
H$_2$ (50 MPa)	15.2	22.8	16.3	0.7
H$_2$ (100 MPa)	15.2	27.0	19.4	0.7
O$_2$ (30 MPa)	3.8	5.6	7.4	1.3
H$_2$O (70 MPa)	5.1	10.7	11.9	1.1
CO$_2$ (30 MPa)	3.2	5.4	8.0	1.5
CO$_2$ (90 MPa)	3.2	8.1	9.3	1.2
CH$_4$ (20 MPa)	5.4	7.9	11.0	1.4
C$_2$H$_6$ (20 MPa)	3.9	7.0	12.0	1.7
CO (20 MPa)	4.1	12.0	7.7	0.6

particular importance from the point of view of governing nuclear reactions, synthesis in stars and the creation of planets, and heavier elements including carbon. The balance between the two dimensionless constants provides a narrow "habitable zone" where stars and planets can form, and life-supporting molecular structures can emerge [28].

B. Comparison to the experimental data

We now compare our bounds to experiments. In Table I we compare α_m calculated according to (11) to the experimental α_m [21] for all liquids shown in Fig. 1. The ratio between experimental and predicted α_m is in the range of about 0.9–4. The ratio is the largest for fluids under high pressure (e.g., N$_2$ at 500 MPa and Ar at 100 MPa), which our Eq. (11) does not account for, as discussed below. For the lightest liquid, H$_2$, experimental α_m is close to the theoretical fundamental thermal diffusivity viscosity (13). We therefore find that (11) predicts the right order of magnitude of α_m.

We observe that α increases with pressure in Table I, similarly to κ in Fig. 1. However, the pressure dependence is not accounted for in α_m in (11) since (11) is derived in the approximation involving Eqs. (7)–(10), which do not account for the pressure dependence of ω_D and E.

We make three further remarks regarding the comparison of theoretical and experimental results in Table I. First, the important term in Eq. (11) includes the combination of fundamental constants that sets the characteristic scale of the lower bound of thermal diffusivity, whereas the numerical factor in (11) may be affected by the approximations used as discussed earlier. Second, Eqs. (7)–(9) assume valence electrons setting strong bonding such as covalent and ionic. Thermal conductivity of these systems in the supercritical state is unavailable due to high critical points. The available data [21]

used in Fig. 1 and Table I include weakly bonded systems such as molecular, noble, and hydrogen-bonded fluids. Bonding in these systems is also electromagnetic in origin, although weak van der Waals and dipole interactions result in smaller E and, therefore, smaller α. However, we note that the dependence of α_m on bonding type is weak because (i) α_m in (10) contains the factor Ea^2, and (ii) a is two to four times larger and $E^{\frac{1}{2}}$ is three to ten times smaller in weakly bonded as compared to strongly bonded systems [29]. As a result, the order-of-magnitude evaluation (11) is unaffected, as Table I shows. Third, Eq. (11) for strongly bonded nonmetallic (covalent and ionic) fluids gives a *prediction* for future experimental work.

The lower bound setting α_m in (11) is consistent with the uncertainty principle. As discussed earlier, the minimum of α can be evaluated as $\alpha_m = va = \frac{pa}{m}$, where p is the particle momentum. Using the uncertainty relation applied to a particle localized in the region set by a, $\alpha_m \geqslant \frac{\hbar}{m}$. $\frac{\hbar}{m}$ is smaller than α_m in (11) by the factor $F = \frac{1}{4\pi}(\frac{m}{m_e})^{\frac{1}{2}}$. $F \approx 22$ in Ar and becomes smaller for lighter systems. Therefore, the minimum (13) provides a stronger bound as compared to the uncertainty relation.

An important difference of our lower bound (11) and bounds based on the uncertainty relations in earlier discussions [3–10] is that (11) corresponds to a true minimum of thermal diffusivity, as seen in Fig. 1 (in the sense that the function has an extremum), whereas the uncertainty relation compares a product (px or Et) to $\hbar$ but the product does not necessarily correspond to a minimum of a function, and it can apply to a monotonic function.

C. Energy and momentum diffusion

We now discuss the relationship between the minima of α and the minima of kinematic viscosity v, v_m. Interestingly, the question of viscosity minima was raised before. Purcell observed [30] that "viscosities have a big range but they stop at the same place." In the earlier work, we have ascertained the lower limit of kinematic viscosity in terms of fundamental constants [16].

We plot the experimental α and v for two noble and two molecular liquids in Fig. 2 at the same pressure as in Fig. 1. We observe the closeness of the minima of both properties. This is unexpected and is surprising, in view of the fact that the two properties are physically distinct and are measured very differently. We compare α_m and v_m below in detail.

There are interesting and important similarities and differences between the two properties. The first analogy is that Eq. (1), which describes energy diffusion, is analogous to that determining momentum diffusion if T is replaced by the velocity field and α is replaced by v. Second, recall that the minimum of thermal conductivity is due to v and l changing from the phonon speed and phonon mean free path in the low-temperature liquidlike regime to particle thermal speed and particle mean path in the high-temperature gaslike regime. The minimum of liquid viscosity is due to the crossover between the exponential decrease of viscosity in the low-temperature liquidlike regime $\eta \propto \exp(\frac{U}{T})$ to $\eta \propto \rho v l$ in the high-temperature gaslike regime, where U is the activation barrier for diffusive particle rearrangements, and v and l are particle thermal speed and mean free path, respectively.
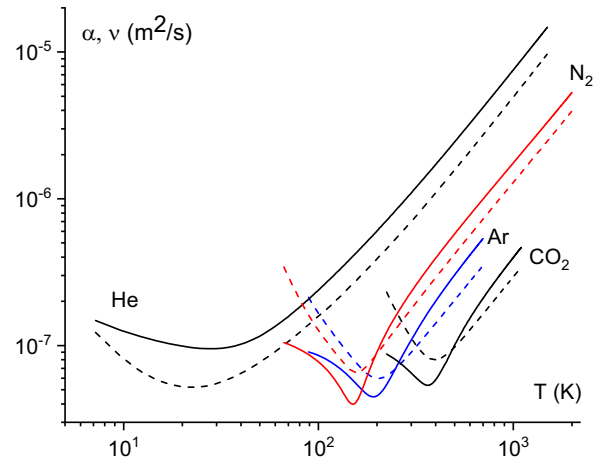

FIG. 2. Experimental α (solid lines) and v (dashed lines) for He (20 MPa), N_2 (10 MPa), Ar (20 MPa), and CO_2 (30 MPa) [21].

Therefore, the temperature dependence of the thermal conductivity and the viscosity is the same in the gaslike regime at high temperature but is different in the liquidlike regime at low temperature. Third and finally, the dominant contribution to thermal conductivity in the low-temperature liquidlike regime is due to phonons as in solids. In the high-temperature gaslike regime, thermal conductivity is due to particle collisions. Viscosity, on the other hand, is due to the dynamics of individual particles and momentum they transfer in both liquidlike and gaslike regimes. Therefore, thermal conductivity and viscosity are set by the same process at high temperature but by different processes at low. Consistent with this picture, Fig. 2 shows that the temperature behavior of α and v is more similar at high temperature as compared to low.

Despite the above differences between α and v, theoretical values at their *minima* are the same. Indeed, we have previously shown [16] that the minima of v (v_m) are given by Eq. (6) or Eq. (11) involving fundamental physical constants, implying

$$v_m = \alpha_m. \tag{15}$$

Therefore, the closeness between v_m and α_m is explained by observing that both α and v at their minima are governed by UV properties such as Bohr radius and Debye frequency in Eq. (6).

We have calculated $v = \frac{\eta}{\rho}$ using the experimental values of viscosity η and density ρ [21] for all liquids at the same pressure as thermal conductivity in Fig. 1, and we show the minima of v (v_m) in the third column in Table I. We observe that the experimental values of α_m and v_m are close to each other. This agreement is also seen in the last column of Table I where the ratio v_m/α_m is in the range 0.4–1.7. We note that the temperatures of the minima of α_m and v_m are somewhat different, nevertheless the closeness of α_m and v_m implies that the Prandtl number, $\frac{v}{\alpha}$, is on the order of 1 at temperatures close to the minima. This is seen in the last column of Table I.

The agreement between experimental α_m and v_m as well as their agreement with the theoretical estimation in the first column in Table I importantly reinforces our analysis of the minima and adds to its consistency.
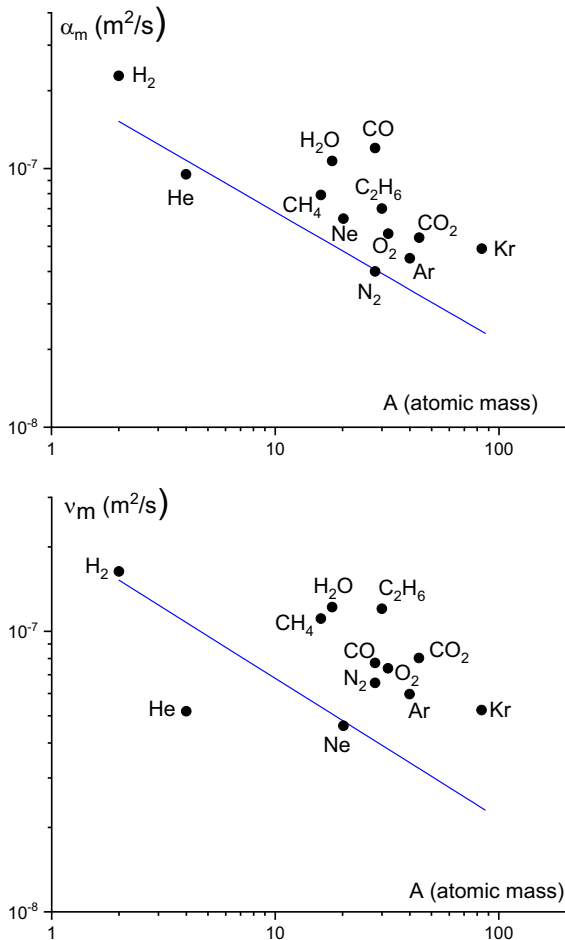
FIG. 3. Points show experimental α_m (top) and ν_m (bottom) as a function of molecular mass. The solid line is the prediction of Eq. (11).

Our final comparison of the theoretical result and experimental data concerns the inverse square-root dependence of α_m and ν_m: according to Eqs. (11) and (15), $\alpha_m, \nu_m \propto \frac{1}{\sqrt{m}}$. Figure 3 shows the experimental α_m and ν_m of all systems in Table I at low pressure as a function of the molecule mass, together with the solid line representing the theoretical result (11). We observe a trend of both α_m and ν_m reducing with molecular mass. We also observe that nearly all experimental plots are above the theoretical prediction of the lower bound. We note that the inverse square-root dependence is expected for strong electromagnetic interactions where energy and interatomic distance do not depend on the ion mass. For weak interactions, the energy depends on the size of the atom or molecule [29]. This contributes to the scatter of points in Fig. 3.

We note that the above discussion applies to systems where the dominant contribution to thermal diffusivity is related to the motion of ions rather than electrons [the electron mass m_e enters Eq. (11) because m_e enters the Bohr radius (7) and Rydberg energy (8)]. The minima of α due to electrons will be discussed elsewhere. Here, we note that thermal conductivity of both high-temperature solid and liquid metals is typically in the range 10–100 $\frac{W}{mK}$ and two to three orders of magnitude

higher than in insulators [31] due to the electronic contribution (this is related to smaller electron mass compared to ion mass.) Hence the minimum discussed here applies to conducting systems, too.

D. Minima on the phase diagram

α_m provides a useful guidance for the minimal value of thermal diffusivity achieved for a given material. This can be important, for example, in the area of thermal insulation. Small values of thermal conductivity are also important in other areas, such as enhancing the thermoelectric effect. As already noted, the exceptionally low thermal conductivity reported in Ref. [27] for the solid with a high thermoelectric figure is still larger than the minima of κ in Fig. 1(a).

It is interesting to ask whether the minima of ν_m and α_m discussed for the liquid and supercritical states apply to other parts of the phase diagram. In solids, $\alpha = vl$ in Eq. (4) is larger because (i) the speed of sound v is faster and (ii) the mean free path l is larger than that in liquids and is typically larger than a at the UV cutoff. It can be seen that vl similarly increases in gases if we recall that the minima at the UV cutoff approximately correspond to the Frenkel line [18,25,26]. The speed of sound is approximately equal to the thermal speed of particles at the line, and it increases above the line in the gaslike state as thermal velocity $\propto \sqrt{T}$. l becomes the particle mean free path above the line in the gaslike state and similarly increases with temperature. Hence, $\alpha = vl$ increases in gases, and the minimum of α, α_m at the UV cutoff, applies to all three states of matter.

The minima α_m and ν_m behave differently in close proximity to the critical point. Indeed, viscosity diverges at the critical point [32], and ν_m increases close to the critical point. Therefore, ν_m gives the global minimum on the entire phase diagram. On the other hand, isobaric heat capacity diverges much faster than κ [33], and α at the critical point tends to zero as a result. Therefore, α_m gives the minimum on the phase diagram except in the vicinity of the critical point.

III. CONCLUSIONS

In summary, we have shown that thermal diffusivity of liquids and supercritical fluids has a lower bound that is fixed by fundamental physical constants for each fluid. The newly introduced elementary thermal diffusivity has an absolute lower bound dependent on $\hbar$ and the proton-to-electron mass ratio only. We have also shown that (i) the lower bound of thermal diffusivity theoretically coincides with the lower bound of kinematic viscosity, and (ii) the ratio between experimental minima of the two properties is close to 1. This finding implies a universal lower bound for two distinct properties—energy and momentum diffusion—which, to the best of our knowledge, has not been discussed before.

[1] N. Ashcroft and N. Mermin, *Solid State Physics*, HRW International Editions (Saunders College, Philadelphia, 1976).

[2] S. Chapman, T. Cowling, D. Burnett, and C. Cercignani, *The Mathematical Theory of Non-uniform Gases: An Account of the Kinetic Theory of Viscosity, Thermal Conduction and Diffusion in Gases*, Cambridge Mathematical Library (Cambridge University Press, Cambridge, 1990).

[3] J. Zaanen, Planckian dissipation, minimal viscosity and the transport in cuprate strange metals, Sci. Post. Phys. **6**, 061 (2019).

[4] C. H. Mousatov and S. A. Hartnoll, On the Planckian bound for heat diffusion in insulators, Nat. Phys. **16**, 579 (2020).

[5] K. Behnia and A. Kapitulnik, A lower bound to the thermal diffusivity of insulators, J. Phys.: Condens. Matter. **31**, 405702 (2019).

[6] Y. Machida, N. Matsumoto, T. Isono, and K. Behnia, Phonon hydrodynamics and ultrahigh–room-temperature thermal conductivity in thin graphite, Science **367**, 309 (2020).

[7] G. Policastro, D. T. Son, and A. O. Starinets, The Shear Viscosity of Strongly Coupled N=4 Supersymmetric Yang-Mills Plasma, Phys. Rev. Lett. **87**, 081601 (2001).

[8] S. A. Hartnoll, Theory of universal incoherent metallic transport, Nat. Phys. **11**, 54 (2015).

[9] C. Luciuk, S. Smale, F. Böttcher, H. Sharum, B. A. Olsen, S. Trotzky, T. Enss, and J. H. Thywissen, Observation of Quantum-Limited Spin Transport in Strongly Interacting Two-Dimensional Fermi Gases, Phys. Rev. Lett. **118**, 130405 (2017).

[10] J. Zaanen, Superconductivity: Why the temperature is high, Nature (London) **430**, 512 (2004).

[11] M. Blake, Universal Charge Diffusion and the Butterfly Effect in Holographic Theories, Phys. Rev. Lett. **117**, 091601 (2016).

[12] M. Baggioli and W.-J. Li, Universal bounds on transport in holographic systems with broken translations, Sci. Post. Phys. **9**, 007 (2020).

[13] S. Grozdanov, Phys. Rev. Lett. (in press), arXiv:2008.00888.

[14] D. D. Joseph and L. Preziosi, Heat waves, Rev. Mod. Phys. **61**, 41 (1989).

[15] G. F. Lawler, *Random Walk and the Heat Equation* (American Mathematical Society, Providence, Rhode Island, 2010).

[16] K. Trachenko and V. V. Brazhkin, Minimal quantum viscosity from fundamental physical constants, Sci. Adv. **6**, eaba3747 (2020).

[17] L. D. Landau and E. M. Lifshitz, *Statistical Physics* (Pergamon Press, Oxford, 1969), Vol. 5.

[18] K. Trachenko and V. V. Brazhkin, Collective modes and thermodynamics of the liquid state, Rep. Prog. Phys. **79**, 016502 (2015).

[19] A. Granato, The specific heat of simple liquids, J. Non-Cryst. Solids **307-310**, 376 (2002).

[20] R. B. Bird, W. E. Stewart, and E. N. Lightfoot, *Transport Phenomena* (Wiley, New York, 2002).

[21] National Institute of Standards and Technology database, see https://webbook.nist.gov/chemistry/fluid.

[22] Y. Sun, *Supercritical Fluid Technology in Materials Science and Engineering: Syntheses: Properties, and Applications* (Taylor & Francis, London, 2002).

[23] J. Frenkel, *Kinetic Theory of Liquids* (Oxford University Press, Oxford, 1947).

[24] C. Yang, M. T. Dove, V. V. Brazhkin, and K. Trachenko, Emergence and Evolution of the k Gap in Spectra of Liquid and Supercritical States, Phys. Rev. Lett. **118**, 215502 (2017).

[25] V. V. Brazhkin, Y. D. Fomin, A. G. Lyapin, V. N. Ryzhov, E. N. Tsiok, and K. Trachenko, Liquid-Gas Transition in the Supercritical Region: Fundamental Changes in the Particle Dynamics, Phys. Rev. Lett. **111**, 145901 (2013).

[26] V. V. Brazhkin and K. Trachenko, What separates a liquid from a gas? Phys. Today **65**(11), 68 (2012).

[27] L. D. Zhao *et al.*, Ultralow thermal conductivity and high thermoelectric figure of merit in SnSe crystals, Nature (London) **508**, 373 (2014).

[28] J. Barrow, *The Constants of Nature: From Alpha to Omega—The Numbers that Encode the Deepest Secrets of the Universe* (Pantheon Books, New York, 2002).

[29] V. V. Brazhkin, Interparticle interaction in condensed media: Some elements are more equal than others, Phys. Usp. **52**, 369 (2009).

[30] E. M. Purcell, Life at low Reynolds number, Am. J. Phys. **45**, 3 (1977).

[31] M. E. Drits, *Properties of Elements* (Moscow Metallurgy, Moscow, 1997).

[32] R. F. Berg, M. R. Moldover, and G. A. Zimmerli, Viscoelasticity of Xenon Near the Critical Point, Phys. Rev. Lett. **82**, 920 (1999).

[33] M. A. Anisimov, Fifty years of breakthrough discoveries in fluid criticality, Int. J. Thermophys. **32**, 2001 (2011).